Rietveld refinement using synchrotron powder diffraction data for curcumin, $C_{21}H_{20}O_6$, and comparison with density functional theory

Joel W. Reid,[1,a)] James A. Kaduk,[2] Subrahmanyam V. Garimella,[3] and John S. Tse[3]
[1]*Canadian Light Source, 44 Innovation Boulevard, Saskatoon, SK S7N 2V3, Canada*
[2]*Illinois Institute of Technology, 3101 S. Dearborn St., Chicago, Illinois 60616*
[3]*Department of Physics and Engineering Physics, University of Saskatchewan, 116 Science Place, Saskatoon, SK S7N 5E2, Canada*

(Received 5 July 2014; accepted 25 September 2014)

Synchrotron powder diffraction data from beamline 08B1-1 at the Canadian Light Source have been used to examine the structure of curcumin, a prime component of the Asian spice turmeric. Rigid body refinement, with the application of restraints on distances and angles, was performed with the Rietveld software package GSAS yielding monoclinic lattice parameters of $a = 12.6967(1)$ Å, $b = 7.198\ 52(3)$ Å, $c = 19.9533(2)$ Å, and $\beta = 95.1241(6)°$ ($C_{21}H_{20}O_6$, $Z = 4$, and space group $P2/n$). The refinement was compared with a recent single-crystal structure and *ab initio* results obtained with density functional theory calculations. © *2014 International Centre for Diffraction Data.*
[doi:10.1017/S0885715614001018]

Key words: curcumin, synchrotron, powder diffraction, density functional theory

I. INTRODUCTION

Curcumin, (1E,4Z,6E)-5-hydroxy-1,7-bis(4-hydroxy-3-methoxyphenyl)hepta-1,4,6-trien-3-one, is the principal active component of the spice turmeric, which is a common food additive, pigment, and ingredient for traditional medicines in Asia (Jayaprakasha *et al.*, 2005). Considerable recent attention has been directed to curcumin and structural analogues for their medicinal potential, including anti-inflammatory (Liang *et al.*, 2009), anti-malarial (Mishra *et al.*, 2008), and anti-cancer properties (Mehta *et al.*, 1997; Adams *et al.*, 2004), among others.

The structure of curcumin was originally solved by Tonnesen *et al.* (1982) using single-crystal X-ray data, but some uncertainty surrounded the enol H atom, which was assigned two atomic sites with the occupancy split between them. A more recent single-crystal study by Parimita *et al.* (2007) established a single enol H site nearly symmetrically centered between the O_2 and O_3 atoms. Figure 1 displays

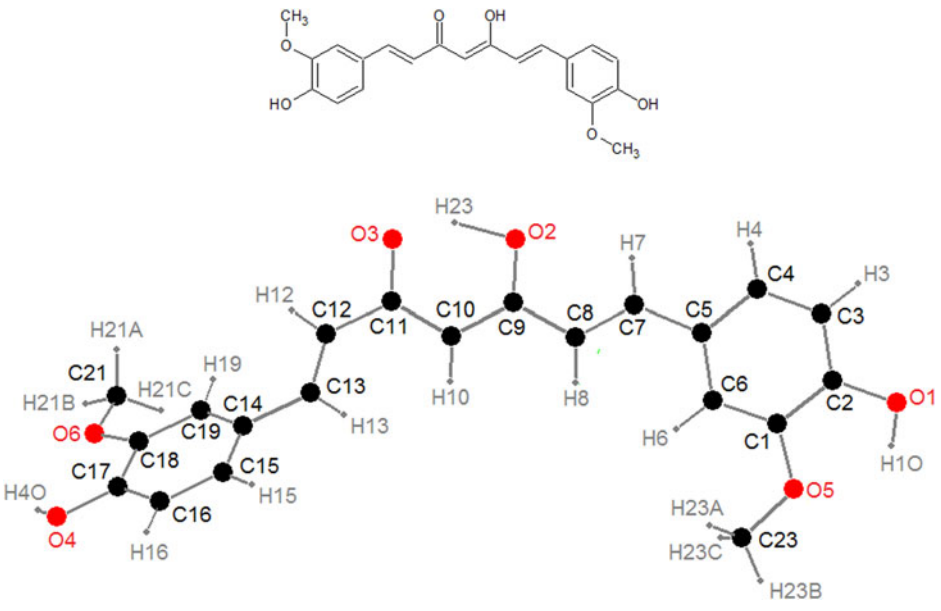

Figure 1. (Colour online) Two 2D diagrams illustrating the molecular structure of curcumin ($C_{21}H_{20}O_6$) and the assigned atom labeling.

a)Author to whom correspondence should be addressed. Electronic mail: joel.reid@lightsource.ca

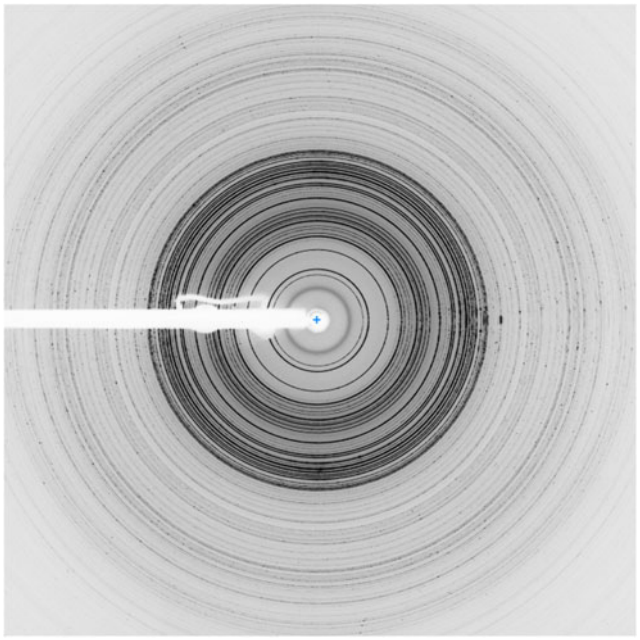

Figure 2. (Colour online) A 2D pattern obtained from curcumin, illustrating the slight graininess of the as-supplied powder.

two illustrations of the curcumin molecule, including the atom labels, which are identical to the site assignments previously defined by Parimita *et al.* (2007).

Despite its usage and investigation for a variety of applications, for many years only one experimental powder diffraction pattern appeared for curcumin in the Powder Diffraction File (PDF 00-009-0816), which is an un-indexed, low precision entry. A new entry 00-063-0943 has been included as a private communication, based on data collected at 100 K and the structure of Form 1 from Sanphui *et al.* (2011). Additional patterns 02-075-3596 and 02-093-7329 are included in the PDF-4 Organics calculated from the crystal structures of Ishigami *et al.* (1999) and Suo *et al.* (2006), respectively. This paper examines the Rietveld refinement of curcumin using rigid body refinement with the Rietveld package GSAS/EXPGUI and provides a comprehensive reflection list for phase identification.

II. EXPERIMENTAL

Curcumin obtained from Sigma-Aldrich (product number C7727) was loaded as-supplied, with no grinding, into a 0.5 mm ID Kapton capillary, which was sealed at both ends with a Loctite adhesive.

Synchrotron powder diffraction (PXRD) patterns were collected using a Canadian Macromolecular Crystallography Facility beamline (CMCF-BM or 08B1-1) at the Canadian Light Source (CLS). 08B1-1 is a bending magnet beamline with an Si (111) double-crystal monochromator. Two-dimensional (2D) data were obtained using a Rayonix MX300HE detector with an active area of 300 mm × 300 mm. The patterns were collected at an energy of 18 keV ($\lambda = 0.688\ 80$ Å) and capillary–detector distance of 350 mm.

The 2D PXRD patterns were calibrated and integrated using the GSASII software package (Toby and Von Dreele, 2013). The sample–detector distance, detector centering and tilt were calibrated using a lanthanum hexaboride (LaB_6) standard reference material (NIST SRM 660a LaB_6) and the calibration parameters were applied to all patterns. After calibration, the 2D patterns were integrated to obtain standard 1D powder diffraction patterns. A pattern from an empty Kapton capillary (collected using the same conditions) was subtracted from the sample data during integration. The integrated LaB_6 pattern was used to obtain the instrument resolution of the beamline for the refinement of the curcumin sample.

The single-crystal structure model of Parimita *et al.* (2007) was used as a starting point for the refinement. The

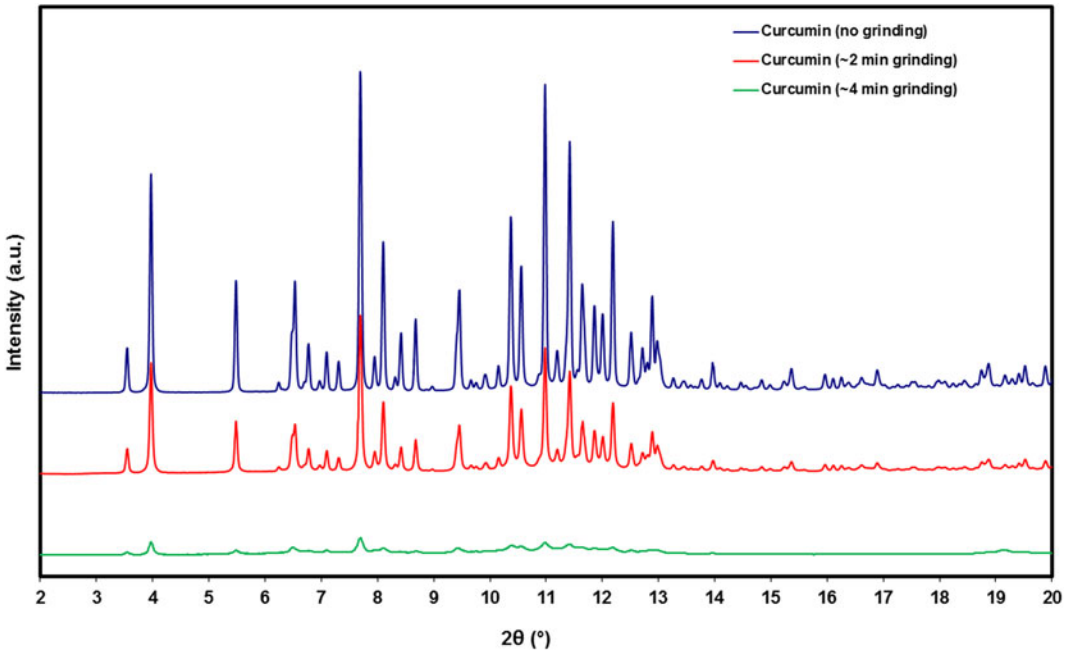

Figure 3. (Colour online) A comparison of the PXRD patterns for curcumin with no grinding (top), ~2 min grinding (middle), and ~4 min grinding (bottom). The patterns were obtained at 18 keV (0.688 80 Å).

https://doi.org/10.1017/S0885715614001018 Published online by Cambridge University Press

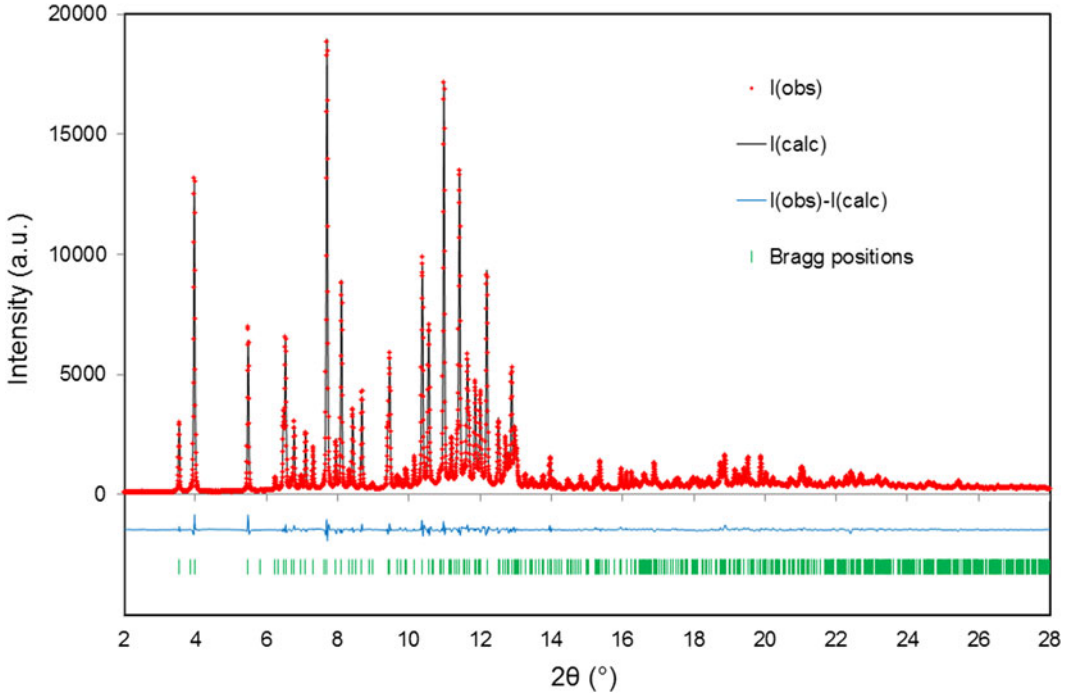

Figure 4. (Colour online) A plot of the final Rietveld refinement obtained for the curcumin sample using GSAS ($\chi^2 = 1.54$).

structure was analyzed with the Mogul 1.6 module of the Cambridge Structural Database (Allen, 2002) in order to prepare appropriate restraints for the distances and angles associated with the carbon and oxygen atoms.

TABLE I. The refined crystal structure of curcumin obtained from the GSAS refinement ($\chi^2 = 1.54$, $R_p = 0.0322$, and $R_{wp} = 0.0428$). The refined lattice parameters obtained are $a = 12.6967(1)$ Å, $b = 7.198\,52(3)$ Å, $c = 19.9533(2)$ Å, and $\beta = 95.1241(6)°$. All atom positions, in space group $P2/n$ (#13), correspond to 4 g Wyckoff sites with occupancies of 1.

Atom	*x/a*	*y/b*	*z/c*	U_{iso} (Å^2)
C_7	1.0131(3)	0.2288(9)	0.4251(2)	0.022(3)
H_7	0.959 55	0.240 57	0.379 72	0.028(4)
C_8	0.9559(3)	0.2416(9)	0.4781(2)	0.023(3)
H_8	0.992 39	0.2381	0.529 84	0.029(4)
C_9	0.8433(3)	0.199(1)	0.4751(2)	0.044(3)
O_2	0.8018(3)	0.1533(7)	0.4161(2)	0.046(2)
H_{23}	0.706 16	0.138 16	0.426 97	0.065(3)
C_{10}	0.7888(3)	0.198(1)	0.5322(2)	0.034(3)
H_{10}	0.827 54	0.232 31	0.581 36	0.043(4)
C_{11}	0.6781(3)	0.159(1)	0.5265(2)	0.060(3)
O_3	0.6319(3)	0.1199(6)	0.4680(2)	0.050(2)
C_{12}	0.6179(4)	0.151(1)	0.5810(2)	0.034(3)
H_{12}	0.542 02	0.077 71	0.572 63	0.044(4)
C_{13}	0.6432(3)	0.2072(8)	0.6478(2)	0.027(3)
H_{13}	0.700 55	0.318 63	0.656 36	0.035(4)
Phenyl 1 rigid body				
C_5	1.126 36(4)	0.2694(4)	0.4214(1)	0.021(3)
C_6	1.1948(2)	0.3121(3)	0.477 43(5)	0.017(2)
C_1	1.3013(1)	0.3348(3)	0.471 48(6)	0.031(3)
C_2	1.341 32(4)	0.3138(4)	0.4091(1)	0.058(4)
C_3	1.2747(2)	0.2732(3)	0.353 43(5)	0.031(3)
C_4	1.1676(1)	0.2511(3)	0.359 51(6)	0.048(3)
H_3	1.3056(3)	0.2581(6)	0.304 54(9)	0.041(4)
H_4	1.1147(2)	0.2190(6)	0.3150(1)	0.062(4)
H_6	1.1642(3)	0.3277(6)	0.526 40(9)	0.022(3)

Continued

Rigid body Rietveld refinement was performed with the GSAS/EXPGUI program (Toby, 2001; Larson and Von Dreele, 2004). The implementation of rigid body refinements in GSAS and EXPGUI have been described previously in the literature (Dinnebier, 1999; Lake and Toby, 2011). Rigid bodies were created for each phenyl group based on the single-crystal atomic coordinates, including the hydrogen atoms, using the centroid of the ring as the rigid body origin. The isotropic displacement parameters (U_{iso}) of the carbon and

TABLE I. Continued

Atom	*x/a*	*y/b*	*z/c*	U_{iso} (Å^2)
O_5	1.3756(2)	0.3774(6)	0.5237(1)	0.065(2)
C_{23}	1.3442(4)	0.3703(9)	0.5904(2)	0.045(3)
H_{23A}	1.285 27	0.478 02	0.596 45	0.059(4)
H_{23B}	1.413 26	0.391 32	0.626 05	0.059(4)
H_{23C}	1.309 65	0.235 27	0.598 04	0.059(4)
O_1	1.4460(2)	0.3378(6)	0.4025(2)	0.054(2)
H_{1O}	1.489 98	0.297 17	0.443 67	0.070(2)
Phenyl 2 rigid body				
C_{14}	0.5768(2)	0.1998(5)	0.699 56(9)	0.044(4)
C_{15}	0.5861(2)	0.3292(3)	0.7504(1)	0.053(3)
C_{16}	0.5239(2)	0.3176(3)	0.803 58(9)	0.040(3)
C_{17}	0.4537(2)	0.1757(4)	0.807 79(9)	0.052(3)
C_{18}	0.4457(2)	0.0411(2)	0.7577(1)	0.055(3)
C_{19}	0.5055(2)	0.0531(3)	0.703 69(9)	0.031(3)
H_{15}	0.6431(3)	0.4418(5)	0.7488(2)	0.069(4)
H_{16}	0.5309(4)	0.4233(5)	0.8427(2)	0.052(4)
H_{19}	0.4971(4)	−0.0513(5)	0.6641(2)	0.040(4)
O_6	0.3830(3)	−0.1055(4)	0.7712(2)	0.071(2)
C_{21}	0.3807(4)	−0.2609(7)	0.7262(3)	0.080(3)
H_{21A}	0.317 08	−0.242 14	0.685 54	0.104(4)
H_{21B}	0.368 55	−0.387 63	0.753 31	0.104(4)
H_{21C}	0.455 58	−0.2687	0.703 99	0.104(4)
O_4	0.3947(3)	0.1637(6)	0.8619(2)	0.064(2)
H_{4O}	0.358 14	0.042 46	0.866 05	0.083(3)

https://doi.org/10.1017/S0885715614001018 Published online by Cambridge University Press

TABLE II. A comparison of selected bond distances and angles obtained from the literature single-crystal refinement (Parimita *et al.*, 2007), the PXRD refinement, and the DFT calculations.

Bond distance (bond angle)	Single crystal (Parimita *et al.*, 2007)	PXRD	DFT
C_5–C_7 (Å)	1.466(4)	1.475(3)	1.454
C_5–C_7–C_8 (°)	129.4(3)	128.7(3)	128.7
C_7–C_8 (Å)	1.320(4)	1.339(4)	1.357
C_7–C_8–C_9 (°)	122.8(3)	123.6(2)	121.6
C_8–C_9 (Å)	1.446(4)	1.457(1)	1.446
C_8–C_9–C_{10} (°)	122.6(3)	121.9(3)	123.7
C_9–O_2 (Å)	1.303(3)	1.291(1)	1.344
C_9–C_{10} (Å)	1.390(4)	1.385(2)	1.387
C_9–C_{10}–C_{11} (°)	121.7(3)	119.8(2)	120.2
C_{10}–C_{11} (Å)	1.401(4)	1.428(3)	1.429
C_{10}–C_{11}–C_{12} (°)	124.6(3)	123.6(2)	122.5
C_{11}–O_3 (Å)	1.282(4)	1.289(1)	1.285
C_{11}–C_{12} (Å)	1.458(5)	1.386(3)	1.463
C_{11}–C_{12}–C_{13} (°)	125.8(4)	129.6(3)	125.6
C_{12}–C_{13} (Å)	1.298(4)	1.390(4)	1.350
C_{12}–C_{13}–C_{14} (°)	125.5(4)	126.4(3)	124.8
C_{13}–C_{14} (Å)	1.487(5)	1.401(4)	1.462
C_2–O_1 (Å)	1.366(4)	1.358(3)	1.354
C_{17}–O_4 (Å)	1.356(4)	1.370(3)	1.357
C_1–O_5 (Å)	1.375(4)	1.376(2)	1.362
C_1–O_5–C_{23} (°)	117.2(3)	118.0(2)	117.8
C_{18}–O_6 (Å)	1.363(4)	1.363(2)	1.367
C_{18}–O_6–C_{21} (°)	118.7(3)	117.5(2)	118.7

oxygen atoms were given the initial values from the single crystal model. Hydrogen atoms were constrained to U_{iso} values of 1.3 times the nearest carbon or oxygen neighbor. The positions of the hydrogen atoms were unrefined but periodically optimized with the Mercury 3.3 module of the Cambridge Structural Database (Allen, 2002). The global weight factor for the restraints was initially set at 100, but lowered in steps to a value of 60 for the final refinement. The restraints contributed 13.8% to the final χ^2. The background was refined using a combination of an orthogonal Chebyschev polynomial (three terms) and Debye scattering function (six terms).

A density functional geometry optimization (fixed experimental unit cell) was carried out using CRYSTAL09 (Dovesi *et al.*, 2005). The basis sets for the H, C, and O atoms were those of Gatti *et al.* (1994). The calculation used 8 *k*-points and the B3LYP functional.

III. RESULTS AND DISCUSSION

A 2D PXRD pattern for curcumin is illustrated in Figure 2, which exhibits mild graininess, suggesting a portion of the crystallite size distribution is larger than optimal and the crystallite statistics deviate from those of an ideal powder. Patterns were also collected after grinding the powder in an attempt to eliminate the graininess; however, the patterns obtained from the ground powder suggest that the crystallinity decreases rapidly with grinding. Approximately 4 min grinding nearly completely eliminated the crystalline reflections, as illustrated by Figure 3, and while grinding for 2 min clearly decreased the crystallinity, it did not completely eliminate the graininess. This type of material is well suited to the current Debye–Scherrer geometry with a large area detector, where large portions of the Debye rings can be integrated to obtain accurate intensity estimates. Although the 2D CCD detector limits the resolution, it is superior for obtaining reasonable intensity estimates compared with point detector or multi-detector/analyzer setups which are designed to optimize resolution. This can be crucial for some molecular compounds

TABLE III. Curcumin hydrogen bonds obtained from the DFT calculations, with PXRD values for the *D*···*A* distances given underneath the DFT values.

Bond	*D*–*H* (Å)	*H*···*A* (Å)	*D*···*A* (Å)	*D*–*H*···*A* (°)	Overlap (*e*)	Energy (kcal mol^{-1})[a]
O_2–H_{23}···O_3	1.045	1.445	2.437 2.487(4)	155.9	0.110	17.6
O_4–H_{4O}···O_2	0.980	1.988	2.874 2.828(5)	149.2	0.036	10.8
O_4–H_{4O}···O_6	0.980	2.208	2.682 2.647(4)	108.3	0.014	7.7
O_1–H_{1O}···O_3	0.979	2.055	2.810 3.032(5)	132.3	0.033	10.2
O_1–H_{1O}···O_5	0.979	2.231	2.681 2.667(4)	106.7	0.018	8.0
C_{23}–H_{23B}···O_1	1.088	2.766	3.521 3.386(6)	126.4	0.007	
C_7–H_7···O_2	1.087	2.377	2.772 2.727(5)	99.4	0.006	
C_{19}–H_{19}···O_1	1.081	2.359	3.401 3.609(4)	161.4	0.020	
C_8–H_8···O_4	1.084	2.483	3.519 3.609(6)	159.5	0.015	
C_6–H_6···O_4	1.083	2.541	3.504 3.656(3)	147.7	0.013	
C_{21}–H_{21A}···O_2	1.092	2.421	3.510 3.585(7)	175.3	0.012	
C_{21}–H_{21C}···O_1	1.092	2.630	3.534 3.571(6)	139.7	0.009	
C_{12}–H_{12}···O_3	1.086	2.721	3.792 3.778(5)	169.1	0.014	

[a]The hydrogen bond energies were calculated from the overlap populations using the correlations of Rammohan and Kaduk (2014).

https://doi.org/10.1017/S0885715614001018 Published online by Cambridge University Press

TABLE IV. The reflection list obtained for curcumin from the Rietveld refinement, including integrated intensities ≥0.6%, after summing reflections closer than 0.02° as multiple reflections and using a weighted average reflection position.

h	k	l	d_{obs} (Å)	$2\theta_{calc}$ (°)	$2\theta_{obs}$ (°)	I/I_{max} (%)	$\Delta 2\theta$ (°)
1	0	−1	11.128 18	3.547	3.547	14.0	0.000
0	0	2	9.937 874	3.972	3.972	65.6	0.000
0	1	0	7.197 886	5.485	5.485	31.1	0.000
2	0	0	6.322 638	6.245	6.245	2.5	0.000
1	0	−3	6.096 396	6.477	6.477	14.9	0.000
1	1	−1	6.044 194	6.533	6.533	31.0	0.000
1	1	1	5.892 827	6.701	6.701	2.3	0.000
0	1	2	5.829 396	6.774	6.774	14.2	0.000
1	0	3	5.664 041	6.972	6.972	3.3	0.000
2	0	−2	5.564 404	7.097	7.097	11.9	0.000
1	1	−2	5.403 216	7.309	7.309	9.3	0.000
2	0	2	5.131 223	7.697	7.697	100.0	0.000
0	0	4	4.968 177	7.950	7.950	10.5	0.000
0	1	3	4.874 521	8.103	8.103	45.1	0.000
2	1	0	4.750 449	8.315	8.315	4.1	0.000
2	1	−1	4.692 427	8.418	8.418	17.0	0.000
2	1	1	4.552 095	8.678	8.678	20.9	0.000
2	1	−2	4.402 24	8.974	8.974	1.4	0.000
3	0	−1	4.200 477	9.406	9.406	11.2	0.000
2	1	2	4.178 316	9.456	9.456	28.4	0.000
0	1	4	4.089 014	9.663	9.663	2.5	0.000
2	0	−4	4.089 014	9.665	9.663	2.5	0.002
3	0	1	4.050 957	9.754	9.754	1.5	0.000
2	1	−3	3.989 351	9.905	9.905	2.5	0.000
1	1	−4	3.977 334	9.935	9.935	2.3	0.000
1	0	−5	3.892 534	10.152	10.152	5.8	0.000
1	1	4	3.809 456	10.374	10.374	53.0	0.000
2	0	4	3.743 603	10.546	10.557	37.9	−0.011
2	1	3	3.743 603	10.558	10.557	37.9	0.001
3	1	0	3.637 451	10.866	10.866	2.2	0.000
3	1	−1	3.627 798	10.895	10.895	1.0	0.000
0	2	0	3.599 145	10.982	10.982	87.7	0.000
0	2	1	3.5416	11.161	11.161	1.2	0.000
3	1	1	3.530 249	11.197	11.197	10.3	0.000
0	1	5	3.479 453	11.361	11.361	9.7	0.000
1	2	0	3.461 838	11.419	11.419	69.8	0.000
1	1	−5	3.420 933	11.545	11.556	3.7	−0.011
3	0	3	3.420 933	11.557	11.556	3.7	0.001
1	2	1	3.396 33	11.640	11.640	27.0	0.000
0	2	2	3.384 161	11.682	11.682	11.9	0.000
3	1	2	3.333 828	11.859	11.859	23.2	0.000
2	1	4	3.324 053	11.894	11.894	2.2	0.000
0	0	6	3.312 398	11.936	11.936	1.8	0.000
1	2	−2	3.293 156	12.002	12.006	22.7	−0.004
1	1	5	3.293 156	12.019	12.006	22.7	0.013
1	2	2	3.244 427	12.187	12.187	48.6	0.000
0	2	3	3.161 733	12.504	12.507	12.4	−0.003
4	0	0	3.161 733	12.508	12.507	12.4	0.001
2	1	−5	3.154 448	12.536	12.536	4.5	0.000
2	2	0	3.127 858	12.642	12.643	1.6	−0.001
2	2	−1	3.111 194	12.711	12.711	11.3	0.000
1	2	−3	3.099 295	12.760	12.760	0.8	0.000
3	1	3	3.089 65	12.800	12.800	7.0	0.000
2	2	1	3.069 116	12.886	12.886	27.1	0.000
3	1	−4	3.048 855	12.971	12.972	12.4	−0.001
2	0	−6	3.048 855	12.975	12.972	12.4	0.003
1	2	3	3.037 896	13.020	13.019	6.8	0.001
3	0	−5	3.030 017	13.053	13.053	1.6	0.000
2	2	−2	3.022 179	13.087	13.087	0.6	0.000
1	1	−6	2.982 25	13.263	13.263	2.8	0.000
2	2	2	2.946 644	13.424	13.424	1.4	0.000
4	0	2	2.937 93	13.464	13.464	1.6	0.000
0	2	4	2.914 873	13.571	13.571	0.9	0.000
1	2	−4	2.873 362	13.768	13.768	2.4	0.000
3	1	4	2.832 823	13.966	13.966	7.5	0.000

Continued

https://doi.org/10.1017/S0885715614001018 Published online by Cambridge University Press

TABLE IV. Continued

h	k	l	d_{obs} (Å)	$2\theta_{calc}$ (°)	$2\theta_{obs}$ (°)	I/I_{max} (%)	$\Delta 2\theta$ (°)
4	1	1	2.832 823	13.972	13.966	7.5	0.006
1	2	4	2.807 818	14.089	14.091	1.8	−0.002
2	1	−6	2.807 818	14.096	14.091	1.8	0.005
4	0	−4	2.782 281	14.221	14.221	0.8	0.000
4	1	−3	2.735 78	14.464	14.464	2.0	0.000
1	0	7	2.718 767	14.555	14.555	1.2	0.000
3	2	1	2.690 638	14.708	14.708	0.6	0.000
0	2	5	2.667 91	14.834	14.834	3.2	0.000
1	2	−5	2.641 703	14.976	14.982	1.5	−0.006
0	1	7	2.641 703	14.985	14.982	1.5	0.003
3	2	2	2.600 631	15.220	15.220	2.0	0.000
4	1	−4	2.595 038	15.253	15.253	1.1	0.000
3	1	5	2.584 259	15.307	15.317	1.3	−0.010
3	2	−3	2.584 259	15.323	15.317	1.3	0.006
1	2	5	2.576 401	15.346	15.364	7.0	−0.018
4	1	3	2.576 401	15.365	15.364	7.0	0.001
5	0	−1	2.537 498	15.601	15.601	0.6	0.000
5	0	1	2.480 623	15.956	15.961	5.3	−0.005
3	2	3	2.480 623	15.968	15.961	5.3	0.007
3	0	−7	2.458 739	16.104	16.104	3.4	0.000
4	1	−5	2.436 646	16.251	16.251	3.9	0.000
5	0	−3	2.436 646	16.252	16.251	3.9	0.001
1	2	−6	2.423 022	16.343	16.343	1.0	0.000
4	1	4	2.416 56	16.387	16.387	2.0	0.000
4	0	−6	2.396 373	16.526	16.526	0.6	0.000
5	1	−1	2.393 21	16.548	16.548	0.7	0.000
2	0	−8	2.385 765	16.600	16.600	2.2	0.000
0	3	1	2.382 203	16.625	16.625	1.8	0.000
4	2	−1	2.375 959	16.659	16.669	1.2	−0.010
4	2	0	2.375 959	16.674	16.669	1.2	0.005
2	1	7	2.368 06	16.725	16.725	1.4	0.000
3	1	6	2.359 236	16.781	16.788	1.1	−0.007
1	3	0	2.359 236	16.801	16.788	1.1	0.013
5	1	1	2.345 505	16.884	16.887	6.3	−0.003
1	3	−1	2.345 505	16.886	16.887	6.3	−0.001
4	2	1	2.340 002	16.926	16.927	1.4	−0.001
2	2	−6	2.326 089	17.029	17.029	1.0	0.000
5	0	3	2.295 452	17.258	17.258	1.3	0.000
5	1	2	2.276 472	17.398	17.403	0.6	−0.005
4	2	2	2.276 472	17.407	17.403	0.6	0.004
2	1	−8	2.263 31	17.494	17.505	2.3	−0.011
3	0	7	2.263 31	17.507	17.505	2.3	0.002
0	3	3	2.255 512	17.562	17.566	2.1	−0.004
4	1	5	2.255 512	17.579	17.566	2.1	0.013
2	3	0	2.243 349	17.662	17.662	0.6	0.000
1	3	3	2.209 23	17.936	17.937	1.4	−0.001
1	0	−9	2.209 23	17.939	17.937	1.4	0.002
2	3	−2	2.203 382	17.985	17.985	2.2	0.000
3	2	5	2.195 633	18.049	18.049	1.1	0.000
4	0	6	2.189 858	18.085	18.097	1.8	−0.012
4	2	3	2.189 858	18.098	18.097	1.8	0.001
2	3	2	2.173 306	18.234	18.236	1.4	−0.002
3	2	−6	2.173 306	18.241	18.236	1.4	0.005
0	3	4	2.159 219	18.343	18.356	1.4	−0.013
3	1	7	2.159 219	18.359	18.356	1.4	0.003
2	2	−7	2.150 045	18.435	18.435	2.2	0.000
2	3	−3	2.145 661	18.473	18.473	0.8	0.000
5	1	−5	2.126 379	18.642	18.642	1.0	0.000
1	3	4	2.115 581	18.732	18.738	5.0	−0.006
4	1	−7	2.115 581	18.741	18.738	5.0	0.003
1	1	−9	2.111 784	18.772	18.772	1.3	0.000
6	0	0	2.107 667	18.809	18.809	1.2	0.000
2	3	3	2.104 673	18.836	18.836	1.8	0.000
4	2	−5	2.101 025	18.860	18.869	7.2	−0.009
6	0	−2	2.101 025	18.876	18.869	7.2	0.007
4	1	6	2.096 291	18.912	18.912	0.7	0.000

Continued

https://doi.org/10.1017/S0885715614001018 Published online by Cambridge University Press

TABLE IV. Continued

h	k	l	d_{obs} (Å)	$2\theta_{calc}$ (°)	$2\theta_{obs}$ (°)	I/I_{max} (%)	$\Delta 2\theta$ (°)
3	3	0	2.084 605	19.012	19.019	0.7	−0.007
5	1	4	2.084 605	19.029	19.019	0.7	0.010
2	3	−4	2.069 406	19.160	19.160	4.4	0.000
5	2	0	2.069 406	19.160	19.160	4.4	0.000
5	2	−2	2.056 013	19.285	19.286	2.7	−0.001
2	1	−9	2.056 013	19.288	19.286	2.7	0.002
5	2	1	2.042 586	19.411	19.414	4.6	−0.003
1	2	−8	2.042 586	19.419	19.414	4.6	0.005
3	0	−9	2.032 013	19.515	19.516	6.0	−0.001
3	2	−7	2.032 013	19.533	19.516	6.0	0.017
6	1	−1	2.029 953	19.536	19.536	1.4	0.000
5	1	−6	2.018 087	19.648	19.652	1.1	−0.004
5	2	−3	2.018 087	19.656	19.652	1.1	0.004
1	2	8	1.995 27	19.878	19.879	7.4	−0.001
6	1	1	1.995 27	19.880	19.879	7.4	0.001
3	1	8	1.981 163	20.018	20.022	3.6	−0.004
4	2	5	1.981 163	20.021	20.022	3.6	−0.001
5	1	5	1.973 748	20.098	20.098	0.8	0.000
5	2	−4	1.961 866	20.221	20.221	2.2	0.000
3	3	−4	1.953 264	20.305	20.311	0.7	−0.006
2	1	9	1.953 264	20.314	20.311	0.7	0.003
1	3	−6	1.935 632	20.495	20.498	0.6	−0.003
5	2	3	1.935 632	20.501	20.498	0.6	0.003
3	2	7	1.915 756	20.713	20.713	2.1	0.000
0	1	10	1.915 756	20.714	20.713	2.1	0.001
4	3	0	1.911 375	20.761	20.761	0.6	0.000
2	2	8	1.904 752	20.834	20.834	1.2	0.000
3	3	4	1.893 071	20.962	20.964	0.8	−0.002
4	3	1	1.893 071	20.967	20.964	0.8	0.003
3	0	9	1.887 995	21.021	21.021	5.0	0.000
2	3	−6	1.885 246	21.050	21.052	2.5	−0.002
4	2	−7	1.885 246	21.054	21.052	2.5	0.002
1	2	−9	1.882 682	21.081	21.081	0.9	0.000
6	1	−5	1.868 662	21.241	21.241	1.6	0.000
6	0	−6	1.854 766	21.402	21.402	0.6	0.000
2	2	−9	1.842 769	21.544	21.543	1.1	0.001
6	2	0	1.817 678	21.831	21.844	0.9	−0.013
4	3	−4	1.817 678	21.851	21.844	0.9	0.007
7	0	−1	1.813 741	21.891	21.892	2.0	−0.001
4	1	8	1.813 741	21.898	21.892	2.0	0.005
6	2	1	1.798 648	22.078	22.078	1.1	0.000
5	2	5	1.782 07	22.275	22.286	3.5	−0.011
1	4	0	1.782 07	22.291	22.286	3.5	0.005
1	4	1	1.772 569	22.407	22.407	3.4	0.000
0	4	2	1.769 918	22.429	22.441	1.5	−0.012
3	2	−9	1.769 918	22.446	22.441	1.5	0.005
2	2	9	1.767 352	22.472	22.474	1.5	−0.002
1	0	11	1.767 352	22.484	22.474	1.5	0.010
1	4	−2	1.757 549	22.601	22.601	0.6	0.000
4	0	−10	1.754 637	22.639	22.639	0.7	0.000
4	3	4	1.752 422	22.668	22.668	1.0	0.000
1	4	2	1.749 908	22.701	22.701	3.1	0.000
5	3	−1	1.742 711	22.786	22.796	1.6	−0.010
1	2	−10	1.742 711	22.805	22.796	1.6	0.009
0	4	3	1.736 697	22.876	22.876	1.2	0.000
7	1	−3	1.730 949	22.946	22.953	0.7	−0.007
3	3	6	1.730 949	22.958	22.953	0.7	0.005
2	4	−1	1.727 83	22.992	22.995	1.2	−0.003
2	1	−11	1.727 83	22.997	22.995	1.2	0.002
0	3	8	1.724 944	23.021	23.034	0.6	−0.013
1	3	−8	1.724 944	23.041	23.034	0.6	0.007
6	2	3	1.720 376	23.096	23.096	1.5	0.000
3	0	−11	1.717 076	23.141	23.141	0.8	0.000
1	4	3	1.715 102	23.168	23.168	2.7	0.000
4	1	−10	1.704 725	23.311	23.311	0.6	0.000
7	1	2	1.700 481	23.368	23.370	1.6	−0.002

Continued

https://doi.org/10.1017/S0885715614001018 Published online by Cambridge University Press

TABLE IV. Continued

h	k	l	d_{obs} (Å)	$2\theta_{calc}$ (°)	$2\theta_{obs}$ (°)	I/I_{max} (%)	$\Delta 2\theta$ (°)
7	1	−4	1.700 481	23.387	23.370	1.6	0.017
2	4	2	1.698 188	23.402	23.402	1.0	0.000
2	4	−3	1.684 773	23.591	23.591	1.0	0.000
3	2	9	1.671 92	23.775	23.775	0.6	0.000
2	4	3	1.664 743	23.879	23.879	0.6	0.000
3	3	−8	1.632 618	24.348	24.356	1.1	−0.008
5	3	−5	1.632 618	24.368	24.356	1.1	0.012
1	4	5	1.617 707	24.576	24.584	1.5	−0.008
4	3	6	1.617 707	24.578	24.584	1.5	−0.006
7	2	−2	1.614 216	24.638	24.638	0.6	0.000
6	2	5	1.607 472	24.740	24.743	1.3	−0.003
7	1	−6	1.607 472	24.743	24.743	1.3	0.000
3	2	10	1.564 429	25.416	25.435	2.7	−0.019
4	4	−1	1.564 429	25.432	25.435	2.7	−0.003

which cannot be mechanically ground without significantly reducing their crystallinity.

The final Rietveld refinement is illustrated in Figure 4, whereas the refined atomic coordinates are shown in Table I. Selected bond lengths and angles are provided in Table II for the single-crystal refinement (Parimita *et al.*, 2007), GSAS PXRD refinement and the density functional theory (DFT) calculations for comparison. The bond lengths are generally comparable between the single-crystal and PXRD refinements, but there are some differences. The root-mean-square (RMS) difference between the heavy atom positions and those of Parimita *et al.* (2007) is 0.110 Å, and the RMS difference between the experimental and DFT structures is 0.176 Å. In particular, the C_{12}–C_{13} and C_{13}–C_{14} bond differ significantly, with the DFT calculated bond lengths falling between the values in both cases. The PXRD refined isotropic displacement parameters do not suggest significant issues with the refinement, and generally show marginal differences from the single-crystal values.

Hydrogen bonds obtained from the DFT calculations are shown in Table III, with the $D\cdots A$ values from the GSAS refinement provided for comparison. The shorter distances (below 3 Å) vary little between the DFT and PXRD results, generally less than 0.05 Å; however, larger differences can be seen between some of the longer distances. Much of the impetus behind the single-crystal study of Parimita *et al.* (2007) was an accurate determination of the position of the enol H atom, H_{23}. The DFT calculations suggest that H_{23} is most closely associated with O_2, whereas the single-crystal results place the H_{23} atom nearly symmetrically between O_2 and O_3 [at distances of 1.26(5) and 1.28(5) Å, respectively].

The final reflection list for curcumin obtained from the GSAS refinement is provided in Table IV. To process the data, adjacent reflections with relative integrated intensities

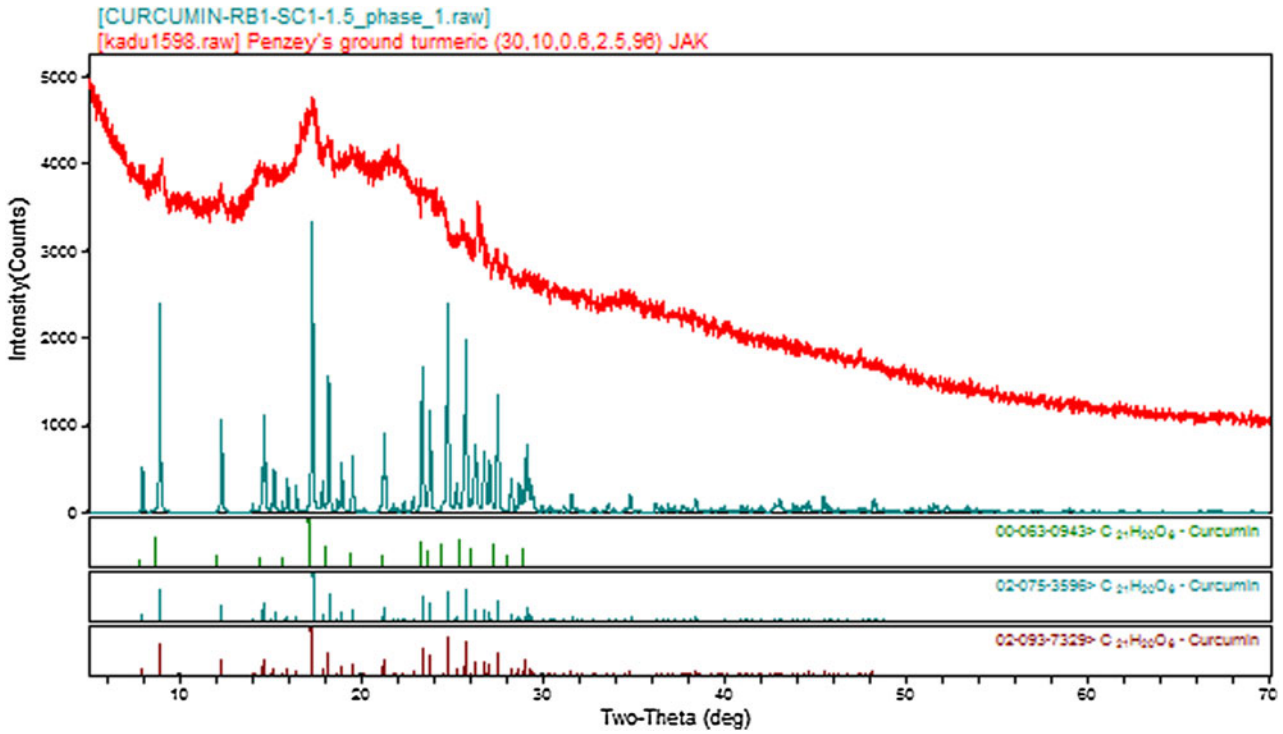

Figure 5. (Colour online) The PXRD pattern obtained from commercial ground turmeric.

https://doi.org/10.1017/S0885715614001018 Published online by Cambridge University Press

larger than 0.2% and closer than 0.02°2θ were summed as multiple reflections and assigned a weighted average reflection position. The final reflection list in Table IV contains all reflections with relative integrated intensities greater than 0.5%.

This curcumin pattern explains well the crystalline peaks in the pattern of commercial ground turmeric (Figure 5). The sample apparently contains a trace of quartz. The peaks of pattern 00-063-0943 (measured at 100 K) are significantly shifted from the experimental peaks and those of the room-temperature calculated patterns 02-075-3596 and 02-093-7329. Anisotropic thermal expansion between 100 and 300 K means that patterns calculated from low-temperature crystal structures are not as useful for phase identification as might be expected, as the peaks are shifted significantly from their positions at ambient conditions. This high-quality powder pattern measured at ambient conditions should prove useful for identification of curcumin using normal powder diffraction techniques.

ACKNOWLEDGEMENTS

Thanks to Dr. Pawel Grochulski for helpful discussions which improved this manuscript. Research described in this paper was performed using beamline 08B1-1 at the Canadian Light Source, which is supported by the Canadian Foundation for Innovation, the Natural Sciences and Engineering Research Council of Canada, the National Research Council Canada, the Canadian Institutes of Health Research, the Government of Saskatchewan, Western Economic Diversification Canada, and the University of Saskatchewan.

SUPPLEMENTARY DATA

The supplementary material for this article can be found at http://www.journals.cambridge.org/PDJ

Adams, B. K., Ferstl, E. M., Davis, M. C., Herold, M., Kurtkaya, S., Camalier, R. F., Hollingshead, M. G., Kaur, G., Sausville, E. A., Rickles, F. R., Snyder, J. P., Liotta, D. C., and Shoji, M. (**2004**). "Synthesis and biological evaluation of novel curcumin analogs as anti-cancer and anti-angiogenesis agents," Bioorg. Med. Chem. **12**, 3871–3883.

Allen, F. H. (**2002**). "The Cambridge Structural Database: a quarter of a million crystal structures and rising," Acta Crystallogr. B **58**, 380–388.

Dinnebier, R. E. (**1999**). "Rigid bodies in powder diffraction: a practical guide," Powder Diffr. **14**, 84–92.

Dovesi, R., Orlando, R., Civalleri, B., Roetti, C., Saunders, V. R., and Zicovich-Wilson, C. M. (**2005**). "CRYSTAL: a computational tool for the *ab initio* study of the electronic properties of crystals," Zeit. Krist. **220**, 571–573.

Gatti, C., Saunders, V. R., and Roetti, C. (**1994**). "Crystal-field effects on the topological properties of the electron-density in molecular crystals – the case of urea," J. Chem. Phys. **101**, 10686–10696.

Ishigami, Y., Goto, M., Masuda, Y., Takizawa, Y., and Suzuki, S. (**1999**). Shikizai Kyokaishi 72, 71; CSD Refcode BINMEQ01.

Jayaprakasha, G. K., Jagan, L., Rao, M. and Sakariah, K. K. (**2005**). "Chemistry and biological activities of *C. longa*," Trends Food Sci. Technol. **16**, 533–548.

Lake, C. H. and Toby, B. H. (**2011**). "Rigid body refinements in GSAS/EXPGUI," Powder Diffr. **26**, S13–S21.

Larson, A. C. and Von Dreele, R. B. (**2004**). *General Structure Analysis System (GSAS)* (Report No. LAUR 86-748). Los Alamos National Laboratory, Los Alamos, NM.

Liang, G., Yang, S., Zhou, H., Shao, L., Huang, K., Xiao, J., Huang, Z., and Li, X. (**2009**). "Synthesis, crystal structure and anti-inflammatory properties of curcumin analogues," Eur. J. Med. Chem. **44**, 915–919.

Mehta, K., Pantazis, P., McQueen, T., and Aggarwal, B. B. (**1997**). "Antiproliferative effect of curcumin (diferuloylmethane) against human breast tumour cell lines," Anti-Cancer Drugs **8**, 470–481.

Mishra, S., Karmodiya, K., Surolia, N., and Surolia, A. (**2008**). "Synthesis and exploration of novel curcumin analogues as anti-malarial agents," Bioorg. Med. Chem. **16**, 2894–2902.

Parimita, S. P., Ramshankar, Y. V., Suresh, S., and Guru Row, T. N. (**2007**). "Redetermination of curcumin: (1E,4Z,6E)-5-hydroxy-1,7-bis(4-hydroxy-3-methoxyphenyl)-hepta-1,4,6-trien-3-one," Acta Crystallogr. E **63**, o860–o862.

Rammohan, A. and Kaduk, J. A. (**2014**). "Structure and bonding in group 1 citrates," manuscript in preparation.

Sanphui, P., Goud, N. R., Khandavilli, U. B. R., Bhanoth, S., and Nangia, A. (**2011**). "New polymorphs of curcumin," Chem. Commun. **47**, 5013–5015.

Suo, Quan-ling, Huang, Yan-chun, Weng, Lin-hong, He, Wen-zhi, Li, Chun-ping, Li, Yun-xia, and Hong, Hai-long. (**2006**). Shipin Kexue (Beijing) 27, 27; CSD Refcode BINMEQ03.

Toby, B. H. (**2001**). "EXPGUI, a graphical user interface for GSAS," J. Appl. Crystallogr. **34**, 210–213.

Toby, B. H. and Von Dreele, R. B. (**2013**). "GSAS II: the genesis of a modern open-source all-purpose crystallography software package," J. Appl. Crystallogr. **46**, 544–549.

Tonnesen, H. H., Karlsen, J., and Mostad, A. (**1982**) "Structural studies of curcuminoids. I. The crystal structure of curcumin," Acta Chem. Scand. B **36**, 475–479.